Isotopic evolution of snowmelt: A new model incorporating mobile and immobile water

Jeonghoon Lee,[1,2] Xiahong Feng,[1] Anthony Faiia,[1] Eric Posmentier,[1]
Randall Osterhuber,[3] and James Kirchner[4,5,6]

Received 16 July 2009; revised 18 June 2010; accepted 6 July 2010; published 4 November 2010.

[1] Isotopic variations of snowmelt provide important information for understanding snowmelt processes and the timing and contribution of snowmelt to catchments in spring. We report a new model for simulating the isotopic evolution of snowmelt. The model includes a hydraulic exchange between mobile and immobile water, and an isotopic exchange between liquid water (mobile and immobile water) and ice within a snowpack. Since this model is based on the mobile-immobile water conceptualization, which is widely used for describing chemical tracer transport in snow, it allows simultaneous simulations of chemical as well as isotopic variations in snowpack discharge. We also report temporal variations of isotopic composition of a snowpack and snowmelt during artificial rain-on-snow experiments and diel snowmelt cycles observed in spring 2003 at the Central Sierra Snow Laboratory, California. These observations are used to test the newly developed model and to understand physical processes in a seasonal snowpack. Our model simulates the isotopic variations reasonably well, and suggests that exchanges of ice with both mobile and immobile water are important for determining the isotopic composition of the discharge.

Citation: Lee, J., X. Feng, A. Faiia, E. Posmentier, R. Osterhuber, and J. Kirchner (2010), Isotopic evolution of snowmelt: A new model incorporating mobile and immobile water, *Water Resour. Res.*, *46*, W11512, doi:10.1029/2009WR008306.

1. Introduction

[2] Models for predicting the chemical and isotopic composition of snowmelt have been used to understand how hydrological processes in catchments influence flow and water quality in stream water, groundwater, and lakes [*Ingraham and Taylor*, 1989; *Theakstone and Knudsen*, 1996; *Williams and Melack*, 1991; *Laudon et al.*, 2002; *Meixner et al.*, 2004]. Modeling the transport of chemical tracers through a snowpack requires a treatment of preferential flow [*Waldner et al.*, 2004], and the simplest model used for this purpose is a mobile-immobile water model (MIM), in which water is partitioned into mobile and immobile components [*van Genuchten and Wierenga*, 1976]. The mobile water advects through a snowpack, carrying solutes with it, while solutes in immobile water can be transported only by exchange with mobile water [*Harrington and Bales*, 1998; *Feng et al.*, 2001; *Lee et al.*, 2008a].

[3] Existing models for simulating the isotopic composition of snowmelt do not consider the isotopic effects of mobile-immobile exchange [*Búason*, 1972; *Taylor et al.*, 2001; *Feng et al.*, 2002]. In the simple model reported by *Taylor et al.* [2001] and *Feng et al.* [2002], all water is mobile and isotopic exchange between liquid water and ice is described as a first-order reaction. While these models are successful in simulating important features of the temporal isotopic evolution of snowmelt, the question of how the mobile-immobile water exchange affects the isotopic composition of snowmelt remains. This is a relevant question, because mobile and immobile water should have different isotopic compositions due to the fact that immobile water has a longer time to exchange with the ice in the snowpack than does mobile water [*Zhou et al.*, 2008]. It would also be advantageous to be able to simulate both chemical and isotopic compositions of a snowpack simultaneously for applications using multiple tracers. In this work, we develop a new model for simulating the isotopic compositions of snowmelt using MIM. This requires that we describe mathematically how the mobile and immobile pools of water exchange with ice when meltwater percolates through a snowpack.

[4] We use two experimental data sets to test the model. The first data set was collected during artificial rain-on-snow storms that were generated over a natural snowpack. The artificial rainwater was isotopically distinct from the snowpack. Chemical tracers were also added to the tap water, and the tracer variations in the discharge have been modeled successfully with a MIM [*Lee et al.*, 2008a]. The best fit mobile-immobile water exchange coefficients have been determined and can be used for the parameterization of

[1]Department of Earth Sciences, Dartmouth College, Hanover, New Hampshire, USA.
[2]Now at Jet Propulsion Laboratory, California Institute of Technology, California, USA.
[3]Central Sierra Snow Laboratory, Soda Springs, California, USA.
[4]Department of Earth and Planetary Science, University of California, Berkeley, California, USA.
[5]Swiss Federal Institute for Forest, Snow, and Landscape Research WSL, Birmensdorf, Switzerland.
[6]Department of Environmental Sciences, Swiss Federal Institute of Technology, Zürich, Switzerland.

0043-1397/10/2009WR008306

the isotopic model. The second set of data consists of diel isotopic variations measured during daily melt cycles in spring 2003.

2. Site Information and Experimental Description

2.1. Field Site

[5] The experiments and observations reported here were made at the Central Sierra Snow Laboratory located at 39°22′19″N, 122°22′15″W, and at an altitude of 2100 m, just west of the crest of the Sierra Nevada near Soda Springs, California. The site conditions have been described in earlier publications [*Feng et al.*, 2001; *Taylor et al.*, 2001; *Unnikrishna et al.*, 2002; *Lee et al.*, 2008a, 2008b]. The snow lab is equipped with two 6 × 3 m^2 melt pans sloped gently to corner drains. One of these melt pans (north pan) was used for our experiments. The discharge from the melt pan is measured by a 4 L data logging tipping bucket. During the winter of our experiments (1 November 2002 to 3 June 2003), the total precipitation was 1450 mm, with 74% of the precipitation falling as snow, and the maximum snow depth was 232 cm (representing 92 cm of snow water equivalent).

2.2. Experimental Methods

[6] Two artificial rain-on-snow experiments were carried out on 5 and 8 April 2003. The artificial rainstorms were generated with two lawn sprinklers, placed about 6 m apart and opposite each other along the bisector of the two 6 m long sides of the melt pan. The inundated area was thus double the width of the pan, thereby minimizing the effects of any lateral flow within the snowpack. Tap water was pumped to the sprinklers from two water supply tanks dug into the snow and lined with plastic sheets. As part of a related study [*Lee et al.*, 2008a], conservative chemical tracers, F^- (KF) and Br^- (LiBr) were mixed into the tanks for the first and second rain-on-snow experiments, respectively, and a sample of the tank water was taken to measure the tracer concentrations and isotopic compositions in the artificial rainwater. The tap water contained a substantial amount of sulfate (~9.4 mg/L), which was significantly higher than the baseline concentration in the snow (~1.1 mg/L). Therefore, sulfate was used as an additional chemical tracer in these experiments [*Lee et al.*, 2008a].

[7] To determine the isotopic composition of the snowpack as a function of depth, we dug pits and sampled snow profiles in an adjacent area on 5 April (at the beginning of the rain-on-snow experiments) and 14 May (two days before the first samples of diel variations in snowmelt). The snow samples were transferred to precleaned (with Citronox®) plastic bags, melted, and transferred to precleaned plastic bottles. Since this study combines isotopic and chemical tracers, both bag and bottles are precleaned. This is not necessary if only isotopic measurements are to be obtained. Liquid water content was measured with a snow surface dielectric device (Denoth meter).

[8] The first rain-on-snow experiment was performed in the afternoon of 5 April; the rainfall lasted 5.1 hours and the amount of rainfall was 157 ± 15 mm (± 1 σ, among measurements from 20 cups). The second simulated storm started in the morning of 8 April, and lasted 5.5 hours with 145 ± 8.5 mm (± 1 σ) of precipitation. These rainfall events are greater than natural rainfalls at this location, both in amount and intensity, although they approach the record 1 day maximum precipitation. We did not attempt to simulate the natural rainfalls in these experiments, but tried to create a distinguishable and observable hydrological event with chemical and isotopic tracers. More detailed information about these experiments can be found in *Lee et al.* [2008a]. An autosampling system for collecting meltwater samples from the north pan upstream of the tipping bucket pumped ~125 mL samples of water into precleaned plastic bottles on a rotating carousel. The absolute sampling times were recorded by an event data logger. We sampled the melt pan discharge every 24 minutes for 2 hours right after the onset of the first simulated rainstorm, and then reduced the sampling frequency to once every 3 hours until the second storm. The sampling rate was then increased to once every 30 minutes for 2 hours on 8 April, at the onset of the second simulated rainstorm, and then decreased to every 3 hours on 9 April, and reduced again to once every 6 hours on and after 10 April. Samples for the study of diel isotopic variations were taken every 3 hours from 16 May to 3 June.

2.3. Isotope Analysis

[9] Each water sample collected during the field experiments was divided into two parts, one for measurements of isotopic ratios and the other for measurement of anion concentrations as reported by *Lee et al.* [2008a]. Samples were analyzed for deuterium/hydrogen (D/H) ratios using an online chromium reduction system (H/device) [*Nelson and Dettman*, 2001], and for $^{18}O/^{16}O$ ratios using the CO_2 equilibration method with a gas bench [*Tu et al.*, 2001]. Both the H/device and the gas bench were interfaced with an isotope ratio mass spectrometer (Thermo-Finnigan Delta+ XL). The memory effect and the fractionation of internal reference gas with time were corrected [*Donnelly*, 2001]. The D/H and $^{18}O/^{16}O$ ratios are expressed in the δ notation as part per thousand differences relative to Vienna Standard Mean Ocean Water (VSMOW). The precisions of the δD and $\delta^{18}O$ measurements were 0.5 and 0.1‰, respectively (1 σ).

3. Mathematical Model

[10] In unsaturated flow with both mobile and immobile water, the fraction of the pore space occupied by water can be denoted by S_w, which in turn can be considered as consisting of two parts: (1) the immobile water S_{im}, and (2) the mobile water, expressed as the "effective water saturation" $S = (S_w - S_{im})/(1 - S_{im})$. An empirical expression for the volumetric flux q_z of meltwater is given by *Colbeck* [1972] as

$$q_z = KS^n, \tag{1}$$

where n is an empirical exponent and K is hydraulic conductivity for saturated flow. Combining equation (1) with mass conservation yields the governing equation for one-dimensional water percolation in the snowpack [*Colbeck*, 1972; *Hibberd*, 1984]:

$$\phi(1 - S_{im})\frac{\partial S}{\partial t} + \frac{\partial (KS^n)}{\partial z} = 0, \tag{2}$$

where ϕ is porosity, z is depth into the snowpack, and t is time. The water percolation velocity, u, is determined by

$$u = \frac{KS^n}{\phi(S_w - S_{im})} = \frac{KS^{n-1}}{\phi(1 - S_{im})}, \quad (3)$$

where $S_w = (1 - S_{im})(S + \beta)$, $\beta = S_{im}/(1 - S_{im})$.

[11] The governing equations for isotopic transport describe advection and dispersion of mobile water, mobile-immobile water exchange, and isotopic exchange between liquid water (mobile and immobile water) and ice [*Wu et al.*, 2004]. The governing equation for isotopic transport in mobile water is

$$\frac{\partial(SC_m)}{\partial t} = \frac{\partial}{\partial z}\left(SD\frac{\partial C_m}{\partial_z}\right) - \frac{\partial}{\partial z}(uSC_m) + \frac{\omega}{\phi(1 - S_{im})}(C_{im} - C_m) + S\frac{(A - C_m)^2}{A} k_r\gamma_m\left(\frac{C_{ice}}{A - C_{ice}} - \alpha\frac{C_m}{A - C_m}\right) \quad (4)$$

where C_m, C_{im}, and C_{ice} are the concentrations of ^{18}O or D in the mobile water, immobile water and ice, respectively (as mass per unit volume), ω is the rate coefficient for exchange between mobile and immobile waters, D is the dispersion coefficient, k_r is the isotopic exchange rate constant, A is 1000 times the ratio of molecular weight of $H_2^{18}O$ over $H_2^{16}O$ (20/18) for ^{18}O concentration or HDO over H_2O (19/18) for D concentration, and α is the oxygen or hydrogen equilibrium fractionation factor between liquid water and ice at 0°C. On right hand side of (4), the first term is the concentration change caused by dispersion, the second term by advection, the third term by hydraulic exchange between mobile and immobile waters, and the last term by isotopic exchange between mobile water and ice. The isotopic exchange term is modified from the expression by *Feng et al.* [2002] by converting the isotopic ratio ($^{18}O/^{16}O$ or D/H) to the absolute concentration of $H_2^{18}O$ or HDO (g/L; e.g., grams of HDO per liter of water of all isotopes). We present the derivations of the isotopic exchange term in the Appendix. Equilibrium fractionation results in $\delta^{18}O$ and δD of water that are 3.1 and 19.5‰ lower, respectively, than those of the ice that is in equilibrium with water [*O'Neil*, 1968]. For isotopic exchange, we assume that the mobile and immobile water pools exchange with separate, non-overlapping fractions of the total mass of ice. This assumption simplifies the mathematical treatment. It may not be entirely valid because some ice may contact both pools of water at different times. However, considering that immobile water is usually present in small pores that are infrequently flushed, the assumption may be largely valid. We use γ_m and γ_{im} to quantify the fractions of ice participating in the isotopic exchanges with the mobile and immobile water, respectively,

$$\gamma_m = \frac{bf_1}{a_m + bf_1} \quad (5a)$$

$$\gamma_{im} = \frac{bf_2}{a_{im} + bf_2}, \quad (5b)$$

with f_1 and f_2 denoting the fractions of ice that are involved in the isotopic exchange with the mobile water and immobile water, respectively, and $f_1 + f_2 \le 1$, which will depend on the accessibility of the ice surface to the infiltrating water. The parameters a_m, a_{im}, and b are the mass of the mobile water, immobile water, and ice per unit volume of snow, respectively, and thus

$$a_m = \phi(1 - S_{im})S\rho_w \quad (6a)$$

$$a_{im} = \phi S_{im}\rho_w \quad (6b)$$

$$b = (1 - \phi)\rho_{ice} \quad (6c)$$

with ρ_w and ρ_{ice} being the density of water and ice, respectively. The f parameters cannot be directly measured and are treated as tuning parameters. *Feng et al.* [2002] discussed physical properties of the parameters and how their values are related to snow processes.

[12] The isotopic composition of immobile water is affected by hydraulic exchange with mobile water and isotopic exchange with ice, and thus the governing equation for immobile water is

$$\frac{\partial C_{im}}{\partial t} = \frac{\omega}{\phi S_{im}}(C_m - C_{im}) + \frac{(A - C_{im})^2}{A} k_r\gamma_{im}\left(\frac{C_{ice}}{A - C_{ice}} - \alpha\frac{C_{im}}{A - C_{im}}\right). \quad (7)$$

The isotopic composition of ice, which is affected by its isotopic exchange with both mobile and immobile water, is governed by

$$\frac{\partial C_{ice}}{\partial t} = (A - C_{ice})^2\left[k_r(1 - \gamma_{im})\left(\alpha\frac{C_{im}}{A - C_{im}} - \frac{C_{ice}}{A - C_{ice}}\right)\right] + \frac{(A - C_{ice})^2}{A}\left[k_r(1 - \gamma_m)\left(\alpha\frac{C_{im}}{A - C_{im}} - \frac{C_{ice}}{A - C_{ice}}\right)\right] \quad (8)$$

Once C_m, C_{im}, and C_{ice} are computed, they can be converted to the corresponding δ values (see Appendix).

4. Experimental Results

4.1. Artificial Rain-on-Snow Experiments

[13] Since the detailed physical and chemical experimental results of the two artificial rain-on-snow experiments have been reported by *Lee et al.* [2008a], we describe only variations in the isotopic ratios in the snowpack and its melt. At the beginning of the rain-on-snow experiments on 5 April, the depth of the snowpack was 210 cm (Snow Water Equivalent (SWE) = 66.5 cm), including 60 cm of new snow that had fallen in the previous 4 days. The snowpack temperature near the snow surface was around −3 to −4°C, increasing with depth to 0°C at about 80 cm below the surface. The $\delta^{18}O$ and δD of the tap water were −10.4 and −79.4‰, respectively. The isotopic ratios in snowmelt before the first artificial rainstorm were −14.3 and −93.0‰ for $\delta^{18}O$ and δD, respectively. The water fluxes and isotopic composition of the discharge as a function of time for the rain-on-snow experiments are shown in Figure 1. The times for the two artificial rainstorms are indicated by the shaded vertical lines labeled in Figure 1a. For each storm, the discharge responded to the rainfall and rose to the level of the input flux. After the storm, water drained gradually from the snowpack. The daily snowmelt also caused the outflow to increase; the daily snowmelt pulses

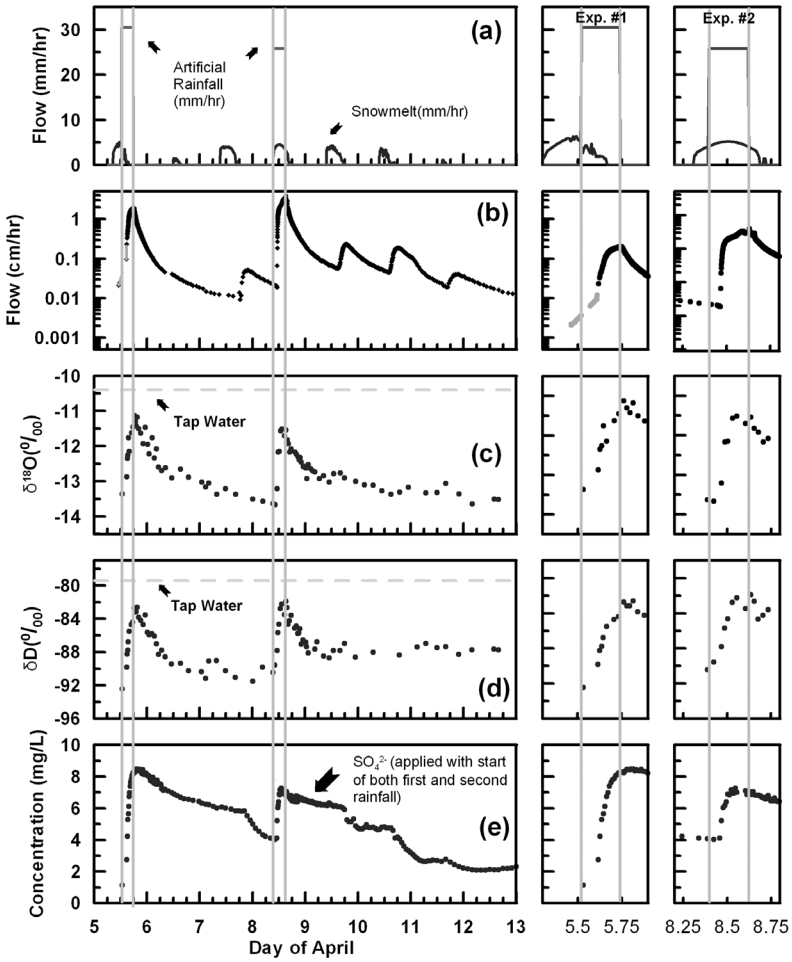

Figure 1. Experimental observations from the two artificial rain-on-snow events. In each row, the left panel shows the 8 day time series, and the two right panels show the two artificial rain-on-snow events with finer scales. The thin shaded lines represent the beginning and end of each experiment. (a) Water input, including artificial rainstorms and calculated snowmelt rates. (b) Water output. The dotted shaded line represents missing flow data resulting from an instrument problem. (c) Oxygen and (d) hydrogen isotopic composition in the discharge. (e) Sulfate tracer concentrations in the discharge from the experiments by *Lee et al.* [2008a]. The δ^{18}O and δD values of the tap water were –10.4 and −79.4‰, respectively, and are marked as shaded lines.

are seen as the smaller input and discharge peaks in Figures 1a and 1b. In Figures 1c and 1d, at the peak flow, the isotopic composition of the snowmelt did not approach as closely to the rain composition as did the concentrations of chemical tracers. The difference is a result of the isotopic exchange between liquid water and ice, which keeps the discharge from reaching the isotopic values of the tap water.

[14] Figures 2a and 2b show snowpack isotopic stratigraphy before and after the first artificial rainstorm. After the first storm, the isotopic compositions of the snowpack about 60 cm from the surface were significantly affected by the artificial rainwater (Figures 2a and 2b). The slope of the regression line on the δD-δ^{18}O diagram in Figures 2c and 2d changed from 8.55 (±0.58) to 6.84 (±0.71), with a change of R^2 value from 0.92 to 0.82, respectively.

4.2. Diel Variations

[15] The depth of the snowpack prior to our sampling for diel variations in snowmelt was 181 cm (SWE = 79.9 cm). On 14 May, the entire snow profile was isothermal at 0°C. The average density of the snowpack was 0.46 ± 0.06 (±1 σ, N = 20), somewhat higher than the density measured prior to the rain-on-snow experiments on 5 April, 0.35 ± 0.14 (±1 σ, N = 23). The increase in average snow density and the decrease in the variability of snow density can be attributed to snow metamorphism, with resulting homogenization of the snowpack. Comparing Figure 3 with Figure 2a, the ranges of δ^{18}O and δD values in the snowpack decreased from 5 April to 14 May. On 5 April, δ^{18}O ranged from −10.6 to −17.2‰ (mean ± standard deviation, −13.1 ± 1.6‰), and by 14 May the range had contracted to −9.5 to −14.0‰ but the average had increased slightly to −11.8 ± 1.2‰. Similarly, on 5 April, δD ranged from −56.1 to −123‰ (mean ± standard deviation, −88.5 ± 14.5‰), and by 14 May the range had reduced to −62.0 to −98.8‰ while the average had increased slightly to −79.7 ± 9.8‰.

[16] The air temperature during our observations from 15 May to 3 June ranged from −6° to 26°C. During this period,

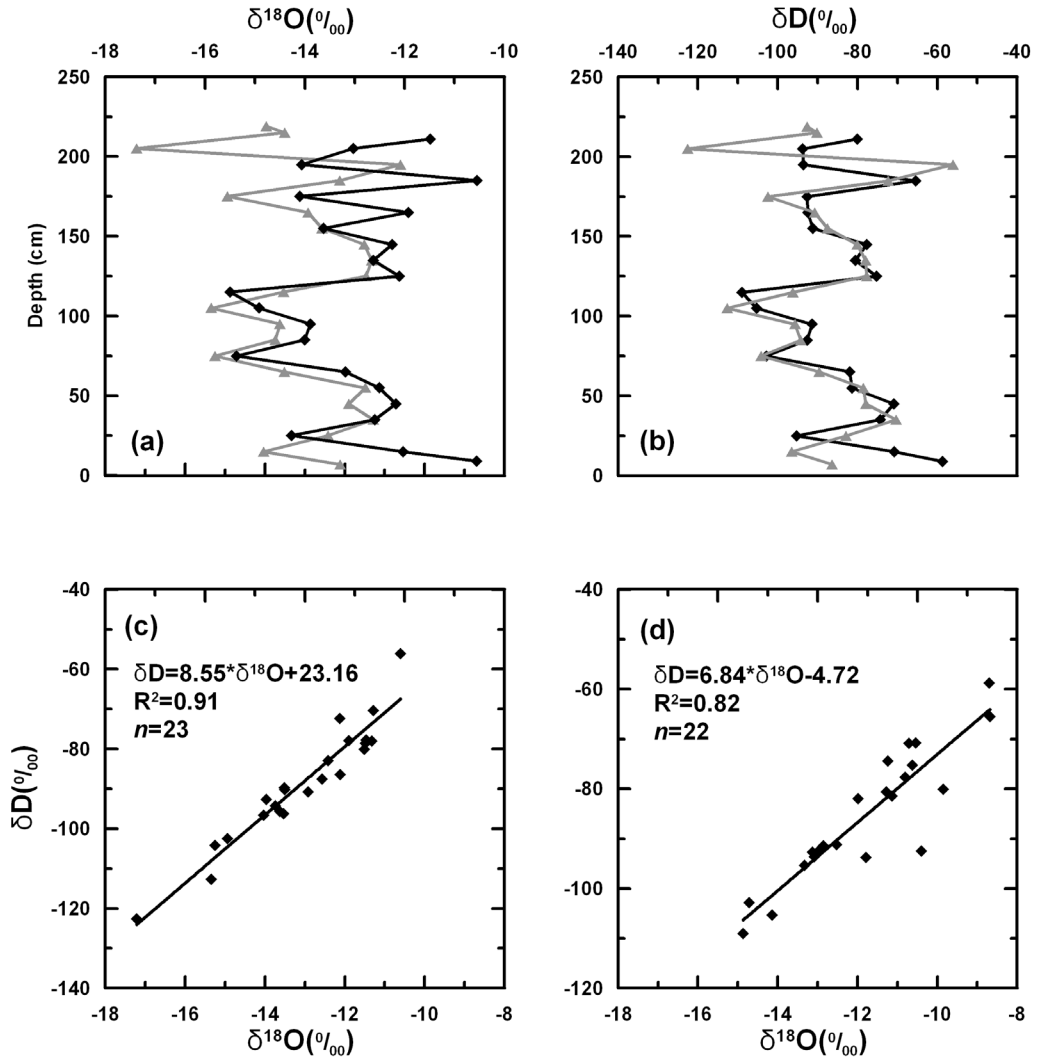

Figure 2. The (a) δ^{18}O and (b) δD variation of the snowpack before (shaded solid line) and after (black solid line) the first rain-on-snow storm, and the δD-δ^{18}O relationship (c) before and (d) after the same storm. The snow pits were dug on 5 April (before the storm) and 6 April (after the storm) 2003.

there was no additional precipitation in the form of either snow or rain. In Figure 4, the flow (mm/hr) and isotopic compositions of meltwater (‰) are plotted as functions of time. The change of snowpack depth (shaded dotted line) is also shown in Figure 4a. For a 24 hour period, the snowmelt discharge can be characterized by a curve with a sharp increase followed by a gradual decrease (a sawtooth shape). Toward the end of the melt season, the amplitude of diel variations of flow increased as the daytime melt rate increased.

[17] There are two notable features in the isotopic compositions of snowmelt in the discharge in Figure 4b. First, there are distinct short-term diel variations (16–22 May) in both oxygen and hydrogen isotopes in the meltwater. Second, the diel variations are superimposed on a weak increasing trend, similar to the trend reported by previous field and laboratory studies [*Herrmann et al.*, 1981; *Taylor et al.*, 2001; *Taylor et al.*, 2002]. There is, however, an abrupt increase in the isotopic ratios near 30 May. This abrupt rise may be attributed to a sharp change in the isotopic profile in the snowpack at a height of about 50 cm, the approximate location of the melting surface on 30 May (Figure 3). The vertical heterogeneity of the snowpack may also result in a disproportionally large isotopic change in the melt water relative to the snowpack. The effect of vertical variation of snowpack on the temporal isotopic evolution in the snowmelt has been discussed in more detail by *Lee et al.* [2010]; we will not discuss this issue further here. Simulations of diel variations will be focused only on the short-term diel isotopic variations from 16 to 22 May (see section 5.2.2.).

5. Results of Numerical Simulations

[18] We used the flow and isotope transport model described in section 3 to simulate the experimental observations. Simulations are done for both rain-on-snow experiments and diel variations of the spring melt.

5.1. Water Flow and Chemical Tracers

[19] The water flow and chemical tracer concentrations have been modeled by *Lee et al.* [2008a]. To make simulations for water flow and chemical tracers, they made four

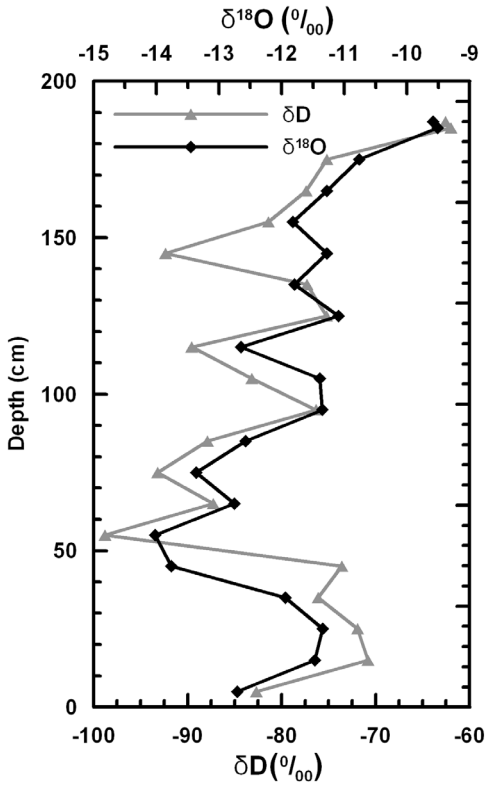

Figure 3. Variations of isotopic compositions of the snowpack collected on 14 May 2003, shortly before the isotopic record in Figure 4 (δ^{18}O, black solid line; δD, shaded solid line).

assumptions about the flow and snowpack conditions, including isothermal snowpack, homogeneous density, and permeability. We adopt their assumptions here and suggest that interested readers refer to their original work for discussions of these assumptions. We apply their best fit parameters of water flow and chemical transport to the isotopic simulation. The exponent (n) and the intrinsic permeability (k) in equation (3) were estimated to be 3 and 52.5×10^{-10} m^2, respectively, for the rain-on-snow experiments. The n and k values used in simulating the diel snowmelt variations were 3 and 75×10^{-10} m^2, respectively. For simulating chemical transport in the rain-on-snow experiment, *Lee et al.* [2008a] used a rate coefficient, ω, that increases linearly with the flow velocity (u) (i.e., $\omega = 3.3 \times 10^{-5}\ u$), to quantify the exchange between mobile and immobile water. Figure 5b shows the model result for water flow, and Figure 5e shows the optimized sulfate simulation from *Lee et al.* [2008a].

5.2. Variations of Snowmelt Isotopes

5.2.1. Artificial Rain-on-Snow Storms

[20] The isotope transport equations (4), (7), and (8) were applied to the snowpack profile to simulate the isotopic compositions of snowmelt reaching the melt pan. The initial isotopic composition of mobile water was assumed to be the same as the isotopic composition of snowmelt before the first application of artificial rainwater (δ^{18}O = −14.3‰ and δD = −93.0‰). The isotopic compositions of both snow and immobile water were assumed to be the measured mean isotopic composition of the snowpack collected on April 5, 2003 (δ^{18}O = −13.1‰ and δD = −88.5‰).

[21] Three key isotopic parameters in the governing equations are the isotopic exchange rate constant between liquid water and ice (k_r), and the mass fractions of ice involved in the isotopic exchange with mobile (f_1) and

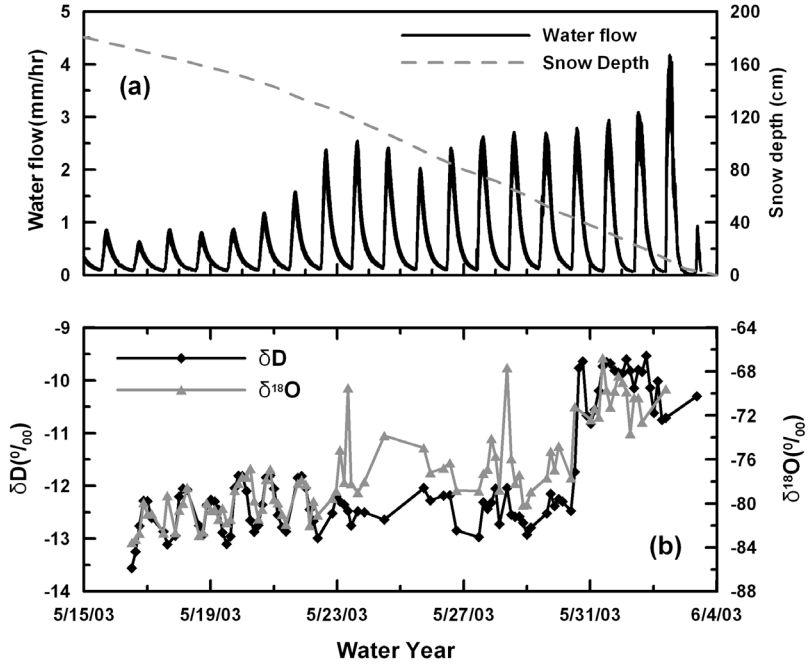

Figure 4. (a) Variations in water flow (black) and snow depth (shaded dotted) during the melting period from 15 May to 4 June 2003. (b) Oxygen (shaded) and hydrogen (black) isotopic variations in snowmelt during the same period.

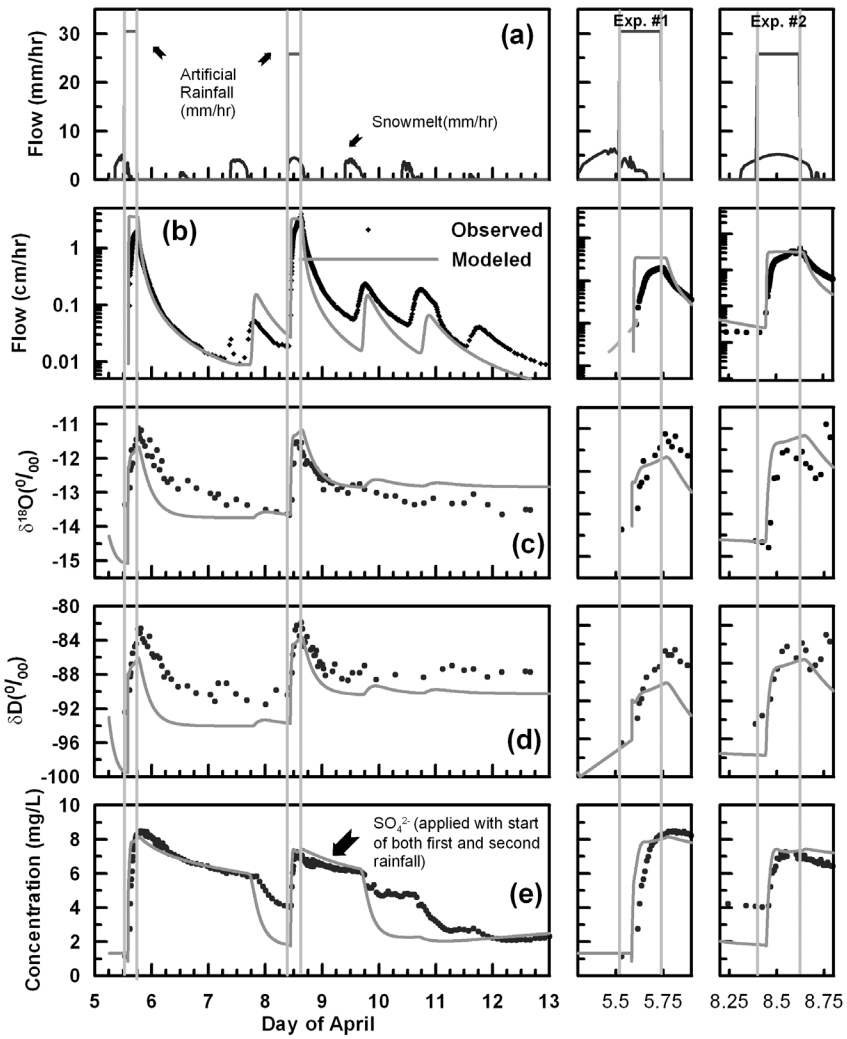

Figure 5. Simulated results (shaded solid lines) and observed data (dots) for the rain-on-snow experiments. (a) Water input and (b) water output with the model result. Simulated (c) δ^{18}O and (d) δD values of snowmelt. (e) Simulated and observed sulfate concentrations from *Lee et al.* [2008a]. The initial isotopic compositions of the mobile water, immobile water, and ice used in the simulations were −14.3‰ (δ^{18}O) and −93.0‰ (δD), −13.1‰ (δ^{18}O) and −88.5‰ (δD), and −13.1‰ (δ^{18}O) and −88.5‰ (δD), respectively.

immobile water (f_2). *Taylor et al.* [2002] determined the isotopic exchange rate constant (k_r) for oxygen to be 0.16 hr^{-1} using a one-dimensional model with three laboratory melting experiments and field data. *Lee et al.* [2009] showed that the exchange rate constants are likely to be the same for oxygen and hydrogen isotopic exchange. The fractions of ice in the exchange were optimized by $f_1 = 0.5$ and $f_2 = 0.4$. As seen in Figures 5c and 5d, the model simulated both isotopes reasonably well using the same set of parameters. As in our previous study, we tried to optimize the model results based on the isotope data of the second storm, because the model assumptions applied better to the snowpack and hydrological conditions (density, porosity, intrinsic permeability, and immobile water content) during the second storm [*Lee et al.*, 2008a].

5.2.2. Diel Variations

[22] We simulated the diel variations of flow and isotopic composition of snowmelt for the period between 17 and 22 May. Figure 6 shows the results of our simulations as functions of time with a uniform initial isotopic composition of the snowpack. The initial isotopic composition of mobile water was assumed to be the same as the isotopic compositions of snowmelt before our calculations started (δD = −79.4‰). The isotopic compositions of both snow and immobile water were assumed to be the measured isotopic composition of the snowpack collected on 14 May (δD = −79.7‰).

[23] In both Figures 6a and 6b, black solid lines represent the observed diel variations and shaded lines represent the model calculations. The simulated water flow reproduced the observed flow reasonably well, although the model calculations underestimated on the declining limbs of the water flow. The isotopic simulation is less impressive, but reveals diel fluctuations. Some inconsistencies between observations and the simulation are from inaccuracies in the discharge flow rate simulations in Figure 6a, others from

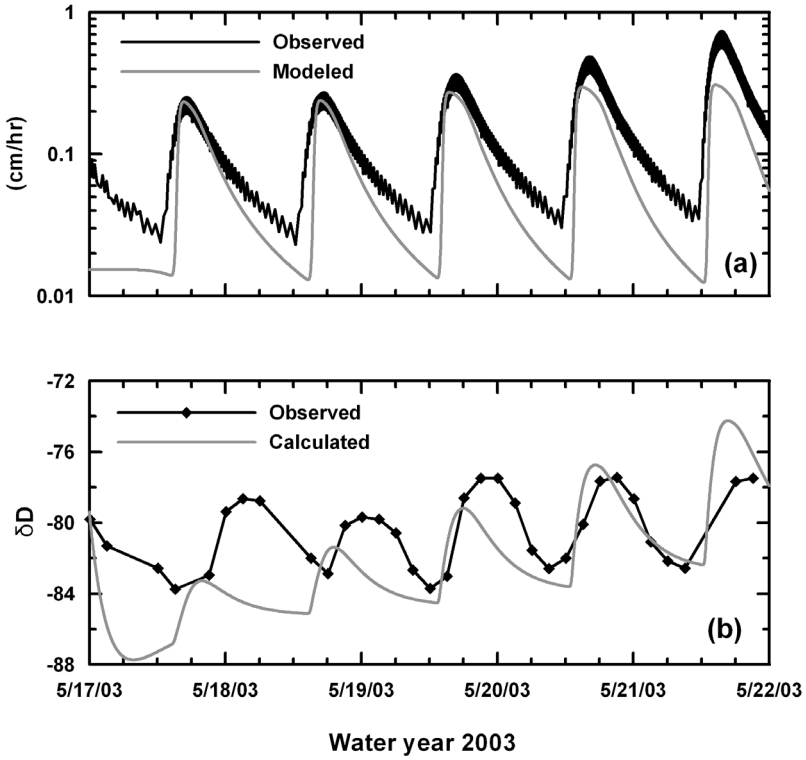

Figure 6. Observed (black lines) and calculated (shaded lines) (a) water flow, and (b) δD of snowmelt under diel melting cycles. For simulations, we used the measured porosity of 0.55, measured bulk density of 0.463 g/cm^3, and 0.04 for S_{im}. The exchange rate between mobile and immobile water was a function of the effective saturation ($\omega = S^2/1.25$) as suggested by *Lee et al.* [2008a]. The initial isotopic compositions of mobile water, immobile water, and ice in this simulation were −79.4, −79.7, and −79.7‰, respectively.

the intrinsic limitations of the model, which we discuss in the next section. The optimized fractions of ice involved in the isotopic exchange were 0.5 for f_1 (mobile water) and 0.025 for f_2 (immobile water).

6. Discussion

[24] The model reproduced the water flow, chemistry, and isotopic compositions of snowmelt reasonably well, suggesting that it includes reasonable representations of the physical processes that control the isotopic variations in snowmelt. The important advance of this model from previous models is its ability to incorporate both mobile-immobile water exchange, which is necessary for simulating chemical variations [*Lee et al.*, 2008a], and liquid-solid isotopic exchange, which controls the isotopic composition of snowmelt. In addition, the model can also reproduce the diel features of the isotopic variations caused by daily melting cycles.

[25] The sensitivity tests for parameterization of water flow and chemical transport have been intensively discussed by *Lee et al.* [2008a], and here we focus only on the role of isotopic exchange between water and ice. We did simulations of oxygen isotopic variations with different f_1 and f_2 values in Figure 7. The hydrological conditions among these simulations are the same as those in Figure 5b. In doing simulations in Figure 7a, we assumed that there was no isotopic exchange between immobile water and ice ($f_2 = 0$). Figure 7b shows how the isotopic exchange between immobile water and ice under a fixed value of f_1 (= 0.5) affects the isotopic composition of snowmelt.

[26] Without the isotopic exchange between immobile water and ice (f_2), we cannot successfully simulate the isotopic composition of snowmelt (Figure 7a), indicating the significance of immobile water in the isotopic exchange system under this model conceptualization. When f_1 increases, the isotopic composition of snowmelt becomes more depleted in ^{18}O until f_1 is 0.5. When f_1 is greater than 0.5, there is no significant further change. The sprayed water is more enriched in ^{18}O compared to all components of the snowpack (initial mobile and immobile water, and ice). As the sprayed water percolates through the snowpack, it pushes the initial mobile water down, while mixing with it (by dispersion). Therefore, the δ^{18}O of the discharge increases as more water is sprayed on to the snow surface. If there were no isotopic exchange between liquid and ice, the discharge would eventually reach the isotopic composition of the tap water (−10.4‰). This did not happen due to isotopic exchange between mobile water and ice. As the f_1 increases, more ice is involved in the liquid-ice isotopic exchange, and discharge becomes more depleted in ^{18}O. However, when f_1 is greater than 0.5, any additional increase in f_1 does not significantly change the fraction of ice in the exchange system (λ_m in equation (6)), because mobile water typically consists of a small mass fraction of the exchange system. As a result, we cannot simulate the observed isotopic depletion by changing f_1 alone.

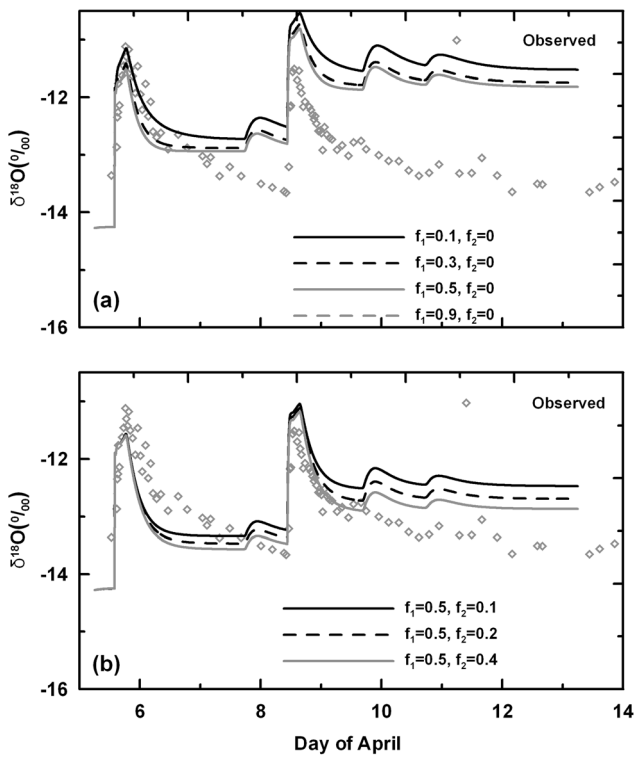

Figure 7. Simulations of oxygen isotopic variations of the discharge during the rain-on-snow experiments based on (a) different fractions of ice participating in the isotopic exchange with mobile water (f_1) and assuming no exchange between ice and immobile water ($f_2 = 0$); and (b) different fractions of ice participating in the isotopic exchange with immobile water under the same value of $f_1 = 0.5$.

[27] When the immobile water begins to participate in the isotopic exchange, results are more realistic. The more the immobile water interacts with ice (f_2 increases), the more depleted the mobile water becomes. The immobile water is depleted in heavy isotopes due to its isotopic exchange with the ice. The mobile water, in turn, can become depleted in heavy isotopes by exchange with the immobile water. In this case, the immobile water is likely to be a source of water depleted in ^{18}O.

[28] Diel variations in the isotopic composition of snowmelt were reported by *Taylor et al.* [2001]. They attributed these variations to changing melt water fluxes in the snowpack, driven by daily variations in the melting rate. When the melting rate is high, water flows through the snowpack with a high velocity, which limits the time of contact between liquid water and ice, thus producing a melt that is closer isotopically to the composition of the melting snow. *Theakstone* [2003] observed diel variations of the isotopic composition of glacier river water in a period of fine weather, but the diel fluctuations were interrupted by rainfall-induced events. Our simulation, although not matching the observations perfectly, does reproduce the diel fluctuations such that the δD of the melt water is higher during a high flow and lower at a low flow. These variations reflect the physical process that the extent of the isotopic exchange between meltwater and ice is relatively high when water flows slowly in comparison to a fast flow condition, and thus less ^{18}O enters the liquid water.

[29] To successfully simulate both the rain-on-snow experiments and the diel cycles, the model required: (1) A greater fraction of ice exchanged isotopes with the liquid water during the artificial rainstorms ($f_1 + f_2 = 0.9$) than during the diel snowmelt cycles ($f_1 + f_2 = 0.525$), and (2) the fraction of ice involved in exchange with mobile water (f_1) greater than the fraction exchanging with immobile water (f_2).

[30] The first result is probably caused by the differences in the wetness and particle sizes of the snowpack at the different times of observation. The artificial rainstorms were conducted early in the season when the snowpack was less metamorphosed than later in the spring when the diel variation was measured. In addition, prior to the rain-on-snow experiments, the snowpack was still accumulating (e.g., there was 60 cm of new snow at the surface). During metamorphism, the grain size of snow increases significantly by recrystallization. Snowpacks with small grain sizes would have a relatively large surface area for the liquid-ice isotopic exchange; the mass of ice involved in isotopic exchange would be increased further by complete dissolution of small particles and their recrystallization onto larger particles. Hydrologically, snowpacks with small grain sizes retain liquid water more effectively, making the snowpack wet, which further enhances snow metamorphism. In our rain-on-snow experiments, the wetness of the snowpack is also enhanced by intensive input of artificial rainwater with fluxes much greater than that from natural snow melting. *Lee et al.* [2009] found a relationship between snow wetness and the fraction of ice involved in the isotopic exchange from laboratory experiments. They argued that, with increasing water saturation in snow, both the surface area of contact between liquid and ice and the rate of dissolution and recrystallization increase. All these arguments points to the possibility that the fraction of ice involved in the isotopic exchange should be higher during the artificial rain-on-snow storms ($f_1 + f_2 = 0.9$) than during the diel snowmelt discharge ($f_1 + f_2 = 0.525$), which is consistent with our model results.

[31] In both simulations, f_1 values were greater than f_2 values. It is not straightforward why this should be the case. One would argue that f_2 should be greater than f_1 because the immobile water may form a thin liquid film around ice grains, making it possible for the immobile water to exchange with a large surface area of ice [*Kutílek and Nielsen*, 1994]. When the water content increases, however, the dead pores may become connected with the mobile water, or thin liquid films that were immobile at a low water content may join the mobile water. In the simulation of diel variations of the melt water, the value f_2 is very small. This result may reflect the fact that, in late spring, ice grain sizes were sufficiently large that little irreducible water was truly immobile. In addition, mobile water may result in more isotopic exchange through dissolution and recrystallization because of wetting of ice grains compared to immobile water where liquid water amount at any given location is limited.

[32] There are still significant discrepancies between the observations and simulations, which are indications of limitations of this model. Some limitations are inherited from

previous models largely due to the assumption of homogenous flow conditions. Others are specific to this isotopic model. Validity for assuming homogeneous density, permeability, and isothermal conditions has been discussed in our earlier work [*Lee et al.*, 2008a]. These assumptions were the reason why our simulation of rain-on-snow experiments was optimized to the second storm, because the assumptions are largely valid to this event. One of the fundamental limitations of the model, as we discussed in several previous contributions [*Feng et al.*, 2001; *Lee et al.*, 2008a, 2008b], is lack of presentation for true preferential flow. Incorporation of mobile and immobile water allows some expression of the fast flow, but it is not sufficient to be compared to the real flow because this model does not allow "immobile" water to have any advective velocity. In addition, the mobile-immobile model does not have kinematic flow. Because of these missing processes, the chemical/isotopic responses to hydrological changes may be too fast, or too slow, or with different magnitude from observations, which cannot be sufficiently corrected by parameterization.

[33] Specific to the isotopic representation of the model, there are also limitations. First, the model assumes that a given mass of ice can only exchange with either mobile or immobile water, but not both, which may not be realistic in natural snowpacks. It is difficult to estimate what bias this limitation would bring to model simulations. On the one hand, when some immobile water becomes mobile as flow rate increases, the complete mixing of mobile water with isotopically depleted immobile water would make the bulk flow depleted in D and ^{18}O. On the other hand, switching of water between mobile and immobile states would decrease the residence time of immobile water, reducing the time of isotopic exchange between immobile water and ice, and thus increasing the isotopic ratio of the immobile water. As a result, hydrological exchange between mobile and immobile water would not result in as much depletion in the bulk flow as if immobile water were truly immobile. Second, the fractions of ice involved in isotopic change, f_1 and f_2, are assumed to be constant for the time period of simulation. This assumption may apply to a mature snowpack, but not to a snowpack undergoing intensive metamorphism with a significant rate of grain growth. Considering these limitations, modeling chemical and isotopic transport in snow remains challenging and calls for further improvements.

7. Summary

[34] We studied temporal variations of snowmelt isotopes using two sets of field observations at the Central Sierra Snow Laboratory, California. First, two artificial rain-on-snow experiments were conducted with tap water more enriched in D and ^{18}O than present in snowmelt prior to the storms. At the peak flow, the isotopic composition of the snowmelt did not approach the rain composition as closely as the concentrations of chemical tracers. Second, later in the spring we collected snowmelt samples every 3 hours, and observed diel variations in the snowmelt isotopic composition as a function of the melting rate.

[35] We developed a new model for simulating isotopic variations in snowmelt. The model is based on the MIM chemical transport model, in that liquid water is partitioned into mobile and immobile fractions. Mobile and immobile water independently exchange with different fractions of the ice. This model allows simultaneous simulation of chemical and isotopic composition of the snowmelt. Here, we demonstrated such an application by simulating both chemical and isotopic variations of discharge from artificial rain-on-snow experiments. The important result from these simulations is the conclusion that the isotopic exchange between immobile water and ice is necessary for reproducing the observed isotopic variations. In particular, without exchange between immobile water and ice, the simulated discharge would not be as depleted in ^{18}O and D as the measurements. The model was also used to simulate diel isotopic variations with a reasonable success. The observed and model results quantitatively demonstrated that the diel isotopic variations are caused by the time of contacts between liquid and ice, which in turn varies with the melting rate of the snowpack.

[36] This model is an important step forward from existing isotope snow models, in that it has some capability for simulating preferential flow. However, the model shares the same limitations as the MIM model; that is, it does not describe true channelized flows and not allowing immobile water to advect with a nonzero velocity. This limitation may be a significant source of mismatch between observations and simulations. In addition, for the isotopic parameterization, the model assumes that mobile and immobile water cannot exchange with the same mass of ice. Moreover, the fractions of ice involved in isotopic change, f_1 and f_2, are assumed to be constant for the time period of simulation. These assumptions may be invalid for snowpacks under certain climate and seasonal hydrological conditions. Although, we do not think these limitations affect the main conclusion of this work, additional efforts are called for to improve the model representation of seasonal snow systems.

Appendix A: Derivations of Isotopic Transport Model

[37] The isotopic exchange kinetics used in the model of this work is adopted and modified from *Feng et al.* [2002]. For example, they used the following equation to quantify the isotopic ratio of ice in exchange with percolating water,

$$\frac{\partial R_{\mathrm{ice}}}{\partial t} = k_r(1-\gamma)\left(R_{\mathrm{ice}} - \alpha R_{\mathrm{liq}}\right), \tag{A1}$$

where R_{ice} and R_{liq} is ^{18}O/^{16}O or D/H ratio in ice and liquid phase of the snowpack, respectively, and t (time), k_r (isotopic exchange rate constant) and α (equilibrium fractionation factor) are defined the same way as our work here. The parameter γ is defined as

$$\gamma = \frac{bf}{a+bf}, \tag{A2}$$

where a and b are mass of water and ice per unit volume of snow, and f is the fraction of ice involved in the isotopic exchange. We show below how we convert the differential equation with respect to the isotopic ratio R to its correspondent concentration of heavy isotopically substituted molecules in water (e.g., gram of HDO per liter of water) using (A1) as an example. The derivation for the three component (mobile, immobile, and ice) model can be

obtained similarly. We first derive the equation for oxygen isotopes using the following

$$R \equiv \frac{^{18}\mathrm{O}}{^{16}\mathrm{O}} = \frac{\mathrm{mole}\mathrm{H_2}^{18}\mathrm{O}}{\mathrm{mole}\mathrm{H_2}^{16}\mathrm{O}}, \tag{A3}$$

$$B_{18} \equiv \frac{\mathrm{mole}\mathrm{H_2}^{18}\mathrm{O}}{\mathrm{mole}\mathrm{H_2}^{16}\mathrm{O} + \mathrm{mole}\mathrm{H_2}^{18}\mathrm{O}} = \frac{R}{1+R}, \tag{A4}$$

$$A_{18} \equiv \frac{20}{18} \times 1000, \tag{A5}$$

and define C_{18} to be the concentration of $H_2^{18}O$ as the grams of $H_2^{18}O$ per liter of water, then

$$C_{18} \approx A_{18}B_{18} \quad \text{or} \quad R = C_{18}/(A_{18} - C_{18}). \tag{A6}$$

From (A6) we obtain

$$\frac{\partial R}{\partial t} = \frac{\partial}{\partial t}\left(\frac{C_{18}}{A_{18} - C_{18}}\right) = \frac{A_{18}}{(A_{18} - C_{18})^2}\frac{\partial C_{18}}{\partial t}. \tag{A7}$$

Introducing (A6) and (A7) to (A1) and adding proper subscripts, we get

$$\frac{\partial C_{18(\mathrm{ice})}}{\partial t} = \frac{(A_{18} - C_{18(\mathrm{ice})})^2}{A_{18}} k_r(1-\gamma)\left(\frac{C_{18(\mathrm{ice})}}{A_{18} - C_{18(\mathrm{ice})}} - \alpha\frac{A_{18_{\mathrm{liq}}}}{A_{18} - C_{18(\mathrm{liq})}}\right). \tag{A8}$$

Once C_{18} is computed, the δ value can be calculated as

$$\delta^{18}O = \left(\frac{C_{18}}{R_{\mathrm{std}}(A_{18} - C_{18})} - 1\right) \times 1000, \tag{A9}$$

where R_{std} is the $H_2^{18}O/H_2^{16}O$ ratio of VSMOW; this ratio is the same as the atomic ratio of $^{18}O/^{16}O$. The derivation for hydrogen isotopes is comparable, except that we need to make two approximations/assumptions. We define the following

$$R \equiv \frac{\mathrm{moleHDO}}{\mathrm{mole}\mathrm{H_2O}}, \tag{A10}$$

$$B_D \equiv \frac{\mathrm{moleHDO}}{\mathrm{mole}\mathrm{H_2O} + \mathrm{moleHDO} + \mathrm{mole}\mathrm{D_2O}} \approx \frac{\mathrm{moleHDO}}{\mathrm{mole}\mathrm{H_2O} + \mathrm{moleHDO}} + \frac{R}{1+R}, \tag{A11}$$

$$A_D \equiv \frac{19}{18} \times 1000. \tag{A12}$$

Equation (A11) is the first approximation in which we consider the amount of D_2O in water as negligible. The derivation for C_D, the concentration of HDO in water, is the same as that of C_{18} shown above. When converting C_D to δD values, the isotope standard is the HDO/H_2O ratio in VSMOW, we assume

$$\frac{\mathrm{HDO}}{\mathrm{H_2O}} = \frac{2\mathrm{D}}{\mathrm{H}}. \tag{A13}$$

This assumption is made for many isotopic determinations using spectral measurements, and is based on the equal probability distribution assumption. It ignores potential quantum effects that cause within-molecule distribution of hydrogen isotopes to deviate from the random distribution.

[38] **Acknowledgments.** This research was partially supported by the National Science Foundation (EAR-9903281, EAR-0111403, and EAR 0418809) and by Dartmouth College.

References

Búason, T. (1972), Equation of isotope fractionation between ice and water in a melting snow column with continuous rain and percolation, *J. Glaciol.*, *11*, 387–405.

Colbeck, S. C. (1972), A theory of water percolation in snow, *J. Glaciol.*, *11*, 369–385.

Donnelly, T., S. Waldron, A. Tait, J. Dougans, and S. Bearhop (2001), Hydrogen isotope analysis of natural abundance and deuterium-enriched waters by reduction over chromium online to a dynamic dual inlet isotope ratio mass spectrometer, *Rapid Commun. Mass Spectrom.*, *15*, 1297–1303.

Feng, X., J. W. Kirchner, C. E. Renshaw, R. S. Osterhuber, B. Klaue, and S. Taylor (2001), A study of solute transport mechanisms using rare earth element tracers and artificial rainstorms on snow, *Water Resour. Res.*, *37*, 1425–1435.

Feng, X., S. Taylor, C. E. Renshaw, and J. W. Kirchner (2002), Isotopic evolution of snowmelt 1: A physically based one-dimensional model, *Water Resour. Res.*, *38*(10), 1217, doi:10.1029/2001WR000814.

Harrington, R., and R. C. Bales (1998), Modeling ionic solute transport in melting snow, *Water Resour. Res.*, *34*, 1727–1736.

Herrmann, A., M. Lehrer, and W. Stichler (1981), Isotope input into runoff systems from melting snow covers, *Nord. Hydrol.*, *12*, 309–318.

Hibberd, S. (1984), A model for pollutant concentrations during snowmelt, *J. Glaciol.*, *30*, 58–65.

Ingraham, N. L., and B. E. Taylor (1989), The effect of snowmelt on the hydrogen isotope ratios of creek discharge in Surprise Valley, California, *J. Hydrol.*, *106*, 233–244, doi:10.1016/0022-1694(89)90074-7.

Kutílek, M., and D. Nielsen (1994), *Soil Hydrology*, Catena Verlag, Reiskirchen, Germany.

Laudon, H., H. F. Hemond, R. Krouse, and K. H. Bishop (2002), Oxygen 18 fraction during snowmelt: Implications for spring flood hydrograph separation, *Water Resour. Res.*, *38*(11), 1258, doi:10.1029/2002WR001510.

Lee, J., X. Feng, E. S. Posmentier, A. M. Faiia, R. Osterhuber, and J. W. Kirchner (2008a), Modeling of solute transport in snow using conservative tracers and artificial rain-on-snow experiments, *Water Resour. Res.*, *44*, W02411, doi:10.1029/2006WR005477.

Lee, J., V. E. Nez, X. Feng, J. W. Kirchner, R. Osterhuber, and C. E. Renshaw (2008b), A study of solute redistribution and transport in seasonal snowpack using natural and artificial tracers, *J. Hydrol.*, *357*, 243–254, doi:10.1016/j.jhydrol.2008.05.004.

Lee, J., X. Feng, E. S. Posmentier, A. M. Faiia, and S. Taylor (2009), Stable isotopic exchange rate constant between snow and liquid water, *Chem. Geol.*, *260*, 57–62.

Lee, J., X. Feng, A. M. Faiia, E. S. Posmentier, J. W. Kirchner, R. Osterhuber, and S. Taylor (2010), Isotopic evolution of a seasonal snowcover and its melt by isotopic exchange between liquid water and ice, *Chem. Geol.*, *270*, 126–134.

Meixner, T., C. Gutmann, R. Bales, A. Leydecker, J. Sickman, J. Melack, and J. McDonnell (2004), Multidecadal hydrochemical response of a Sierra Nevada watershed: Sensitivity to weathering rate and changes in deposition, *J. Hydrol.*, *285*, 272–285, doi:10.1016/j.jhydrol.2003.09.005.

Nelson, S., and D. Dettmam (2001), Improving hydrogen isotope ratio measurements for online chromium reduction systems, *Rapid Commun. Mass Spectrom.*, *23*, 2301–2306.

O'Neil, J. R. (1968), Hydrogen and oxygen isotope fractionation between ice and water, *J. Phys. Chem.*, *72*, 3683–3684.

Taylor, S., X. Feng, J. W. Kirchner, R. Osterhuber, B. Klaue, and C. E. Renshaw (2001), Isotopic evolution of a seasonal snowpack and its melt, *Water Resour. Res.*, *37*, 759–769.

Taylor, S., X. Feng, C. E. Renshaw, and J. W Kirchner (2002), Isotopic evolution of snowmelt: 2. Verification and parameterization of a one-dimensional model using laboratory experiments, *Water Resour. Res.*, *38*(10), 1218, doi:10.1029/2001WR000815.

Theakstone, W. H. (2003), Oxygen isotopes in glacier river waters, Austre Oksindbreen, Okstindan, Norway, *J. Glaciol.*, *49*, 282–298, doi:10.3189/172756503781830700.

Theakstone, W. H., and N. T. Knudsen (1996), Isotopic and ionic variation in glacier river water during three contrasting ablation seasons, *Nord. Hydrol.*, *10*, 523–539.

Tu, K. P., P. D. Brooks, and T. E. Dawson (2001), Using septum-capped vials with continuous flow isotope ratio mass spectrometric analysis of atmospheric CO_2 for Keeling plot applications, *Rapid Commun. Mass Spectrom. 15*, 952–956.

Unnikrishna, P. V., J. J. McDonnell, and C. Kendall (2002), Isotope variations in a Sierra Nevada snowpack and their relation to meltwater, *J. Hydrol.*, *260*, 38–57, doi:10.1016/S0022-1694(01)00596-0.

van Genuchten, M. Th, and P. J. Wierenga (1976), Mass transfer studies in sorbing porous media I: Analytical solutions, *Soil Sci. Soc. Am. J.*, *40*, 473–480.

Waldner, P. A., M. Schneebeli, U. Schultze-Zimmermann, and H. Flühler (2004), Effect of snow structure on water flow and solute transport, *Hydrol. Process.*, *18*, 1271–1290.

Williams, M. W., and J. M. Melack (1991), Solute chemistry of snowmelt and runoff in an alpine basin, Sierra Nevada, *Water Resour. Res.*, *27*, 1575–1588.

Wu, Y. S., H. H. Liu, and G. S. Bodwarsson (2004), A triple-continuum approach for modeling flow and transport processes in fractured rock, *J. Contam. Hydrol.*, *73*, 145–179.

Zhou, S., M. Nakawo, S. Hashimoto, and A. Sakai (2008), Preferential exchange rate effect of isotopic fractionation in a melting snowpack, *Hydrol. Process.*, *22*, 3734–3740, doi:10.1002/hyp.6977.

A. Faiia, X. Feng, and E. Posmentier, Department of Earth Sciences, Dartmouth College, Hanover, NH 03755, USA.

J. Kirchner, Department of Earth and Planetary Science, University of California, 307 McCone Hall, Berkeley, CA 94720, USA.

J. Lee, Jet Propulsion Laboratory, California Institute of Technology, 4800 Oak Grove Dr., M/S 183-601, Pasadena, CA 91109, USA. (jeonghoon.lee@jpl.nasa.gov)

R. Osterhuber, Central Sierra Snow Laboratory, Box 810, Soda Springs, CA 95728, USA.